

Structural Phase Diagrams for the Surface of a Solid: A Total-Energy, Renormalization-Group Approach

J. Ihm,^(a) D. H. Lee, J. D. Joannopoulos, and J. J. Xiong

Department of Physics, Massachusetts Institute of Technology, Cambridge, Massachusetts 02139

(Received 22 February 1983; revised manuscript received 7 September 1983)

Total-energy calculations based on microscopic electronic structure are combined with position-space renormalization-group calculations to predict the structural phase transitions of the Si(100) surface as a function of temperature. It is found that two distinct families of reconstructed geometries can exist on the surface, with independent phase transitions occurring within each. Two critical temperatures representing order-disorder transitions are calculated.

PACS numbers: 68.20.+t, 71.45.Nt

We report a first realistic study of the structural phase transitions of a semiconductor surface at *finite* temperatures. Recent advances in the total-energy-minimization method¹⁻⁸ have made it possible to determine the structure of semiconductor surfaces at *zero* temperature from first principles. The precision of state-of-the-art energy-minimization methods is such that bulk phonon frequencies are reproduced within 10% and relaxed or reconstructed surface geometries can be obtained consistent with existing experimental data. This indicates that the achieved accuracy in the calculation of total-energy differences is better than 10^{-2} eV, a surprising number even in the current standard of solid-state computations.

All calculations, until now, have been restricted to zero-temperature geometries because of the lack of a tractable scheme to incorporate the entropy contribution at finite temperatures. However, if one were able to combine the energy-minimization approach with the renormalization-group technique⁹⁻¹¹ (which has had great success in phase-transition studies for two-dimensional systems) the behavior of semiconductor surfaces at finite temperatures could be predicted quantitatively from first principles. Using a series of approximations described below, we have succeeded in developing such a scheme and applied it to the Si(100) surface, resolving important questions regarding the structure of the Si(100) surface. For example, we show that the (2×1) structure is not the ground state of the Si(100) surface and a higher-order reconstruction should occur on the surface. We predict the disappearance of these higher-order spots roughly above room temperature due to an order-disorder transition. We also obtain a phase diagram for the Si(100) surface which can be used simultaneously for systems belonging to the same universality class such as Ge(100) and diamond (100).

Our basic approximations are summarized as follows. (1) Use of the asymmetric dimer model: Pairs of atoms at the surface relax by dimerizing into one of two possible asymmetric configurations¹ (Fig. 1, inset). Different reconstructions result from different arrangements of asymmetric dimers which are the building blocks of the surface in this model. (2) Use of the tight-binding energy-minimization method: This was first proposed by Chadi.¹ We have included the

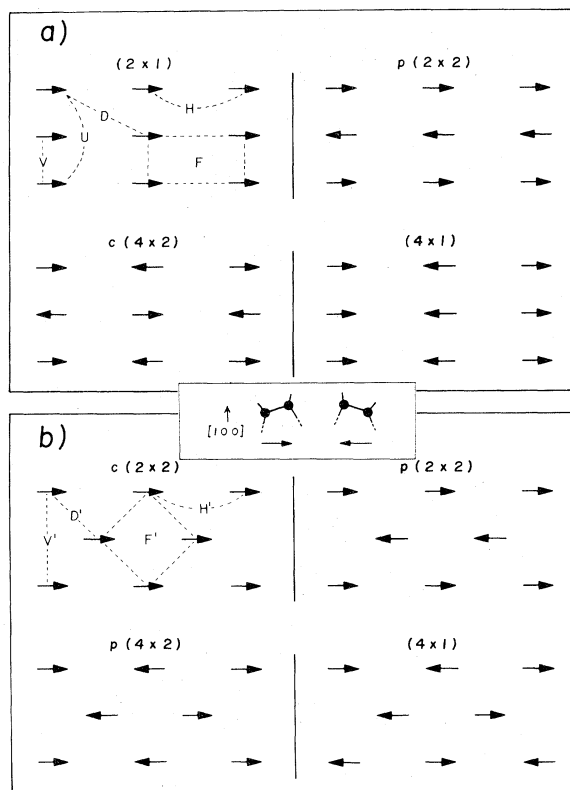


FIG. 1. Reconstruction geometries of the Si(100) surface for (a) " 2×1 " and (b) " $c(2 \times 2)$ " families. Coupling constants for each family are indicated. Side views of the asymmetric dimers are shown in the inset.

excited s orbital in the basis set to improve the accuracy of the calculation.² (3) Mapping onto the spin-one-half Ising Hamiltonian: The two possible orientations of the asymmetric dimer are represented by the two possible states of a spin, and the energy differences between different reconstructions are translated into a set of interaction energies in an effective spin Hamiltonian. (4) Use of the standard position-space renormalization-group method¹⁰ to determine the phase diagrams.

The first and second approximations involve rather controversial issues. For example, the atomic positions on the Si(100) surface are not precisely known. Nevertheless, there is ample experimental support¹² for the asymmetric dimer model and it is the best choice available at present. Next, it is difficult to estimate the precision of the energy differences between different reconstructions obtained from the tight-binding calculations. It is known that the accuracy of the pseudopotential energy calculation is better than 10 meV, but pseudopotential calculations for reconstructed geometries greater than (2×1) or $c(2 \times 2)$ are intractable at the present. After extensive tests and crosschecks with pseudopotential calculations for simpler geometries [(2×1) and $c(2 \times 2)$ structures], we find that the accuracy of the tight-binding energy calculations can be made comparable to that of the pseudopotential method when excited s orbitals are properly included in the basis set. With this extra orbital, we reproduce the energy difference between the symmetric and the asymmetric dimer (0.2 eV)⁴ to within 10 meV and obtain the (2×1) structure lower in energy than the $c(2 \times 2)$ structure, in agreement with both pseudopotential calculations

$$-3\mathcal{C} = V \sum s_{ij} s_{i,j+1} + H \sum s_{ij} s_{i+1,j} + D \sum s_{ij} s_{i+1,j+1} + U \sum s_{ij} s_{i,j+2} + F \sum s_{ij} s_{i,j+1} s_{i+1,j} s_{i+1,j+1},$$

where all interactions up to twice the surface atom spacing are included and illustrated in Fig. 1(a). The couplings U and F contribute equally to the ground-state energies considered here and are taken to be zero. The remaining coupling constants are extracted from the total-energy differences of the individual structures. The total energies at $T = 0$ are calculated with use of the aforementioned tight-binding approach for infinite slabs of Si with twelve-layer thickness. A position-space renormalization-group calculation¹⁰ is then performed, with use of a finite cluster of four cells, each containing five sites. The corresponding flows are in the parameter space of V , H , D , and F only.

and experimental observations. [Without this improvement over Chadi's original scheme, (2×1) would have a higher energy than $c(2 \times 2)$.]

The third approximation is the most natural and simplest to make. A remaining question relates to the number of neighbor interactions that must be included in the effective spin Hamiltonian. In practice, this number is uniquely determined by the number of different reconstruction geometries that need to be compared. Experimentally, higher than quarter-order spots are never observed.¹³⁻²⁰ Thus, the number of possible reconstructions deserving analysis is small (4-5) and can be accommodated by including up to the next-nearest-neighbor interactions in each dimension.

Regarding the fourth approximation, this class of spin systems has been studied extensively and the description of the phase transitions using the renormalization-group approach can be made as accurate as needed.^{10,11}

Let us now turn to the specific problem at hand. Various diffraction experiments¹³⁻²⁰ at room temperature indicate that (2×1) is the basic reconstruction unit for the Si(100) surface. Nevertheless, higher-order spots (up to quarter order) have been seen and, occasionally, a diffuse background as well as streaking is also observed. Whether the ground-state reconstruction of the Si(100) surface is (2×1) or higher has not been resolved experimentally. A family of simple reconstruction geometries with a (2×1) backbone is shown in Fig. 1(a). The spins indicate the two possible asymmetric-dimer orientations. This set of structures will henceforth be called the " 2×1 " family.

The effective "spin" Hamiltonian²¹ for this family may be written as

There is another important family of reconstruction geometries based on a $c(2 \times 2)$ backbone. This family is shown schematically in Fig. 1(b). The interaction parameters for the spin Hamiltonian of this " $c(2 \times 2)$ " family are also illustrated in this figure. These coupling constants are again extracted from total-energy calculations. The coupling F' is taken to be zero for simplicity.

The results of total energies and coupling constants for both families are given in Table I. Several interesting features emerge. In the " 2×1 " family the total energies for the $p(2 \times 2)$ and $c(4 \times 2)$ structures are very similar. Since the error in the theoretical calculations is of the or-

TABLE I. Total energies for various reconstruction geometries with respect to the (2×1) surface and the coupling constants deduced from them.

" 2×1 "	E (meV)	" $c(2 \times 2)$ "	E (meV)
(2×1)	0	$c(2 \times 2)$	67
$p(2 \times 2)$	-36	$p(2 \times 2)$	158
$c(4 \times 2)$	-31	$p(4 \times 2)$	135
(4×1)	36	(4×1)	131
H	10	H'	11
V	-26	V'	-2
D	4	D'	23

der of a few millielectronvolts, it is impossible to tell which structure will actually be realized at very low T . From a practical point of view, surface-preparation conditions dictate the structure to be realized. A typical example is the cleaved Si(111) surface which exhibits a (2×1) structure although the (7×7) structure is believed to be slightly lower in energy. In the " $c(2 \times 2)$ " family the energy difference between structures is much larger. The corresponding phase transition in this family could be predicted with certainty. However, since the $c(2 \times 2)$ structure is significantly higher in energy than the $p(2 \times 2)$ or the $c(4 \times 2)$ structure in the (2×1) family, it is probably not realized under normal conditions. Existence of steps on the surface further hampers the realization of the $c(2 \times 2)$ structure which usually has more dangling bonds across the step and requires more energy to be created. If both (2×1) and $c(2 \times 2)$ families happen to be created on the surface, the domain wall between these two structures is going to be very stable. Breaking or displacing the wall costs a "huge" amount of energy (~ 1.7 eV per dimer). Thus each domain will behave independently, with different phase transitions occurring in each.

The phase diagram for each family is shown in Figs. 2(a) and 2(b), respectively. This is a reduced parameter space obtained by dividing each coupling constant by kT (e.g., $d \equiv D/kT$, $h \equiv H/kT$, etc.). The cross sections of constant d are shown to help visualize the phase space. All phase boundaries shown in the figure are second order. As T increases one moves toward the origin on a straight line in parameter space as indicated in the figure.

For the " 2×1 " family, this diagram shows that a second-order transition occurs between layered-antiferromagnetic $p(2 \times 2)$ and paramagnetic (disordered) phases at roughly 250 K. As we have already mentioned, however, our theoretic

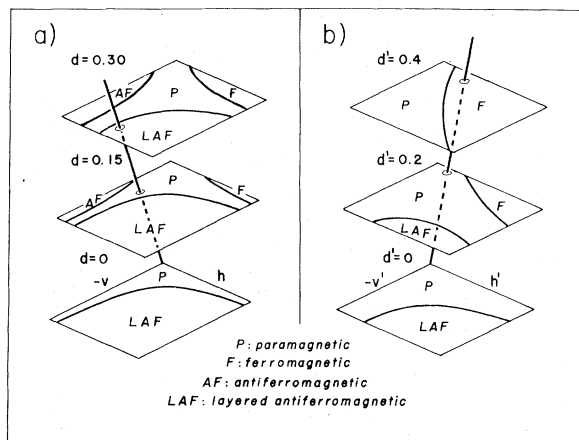


FIG. 2. Phase diagrams in reduced parameter space for (a) " 2×1 " and (b) " $c(2 \times 2)$ " families. The straight lines passing through the origin correspond to the particular set of interaction constants of the Si(100) system at varying temperatures as explained in the text. In (a) F is the (2×1) , LAF is the $p(2 \times 2)$, and AF is the $c(4 \times 2)$ structure. In (b) F is the $c(2 \times 2)$ and LAF is the $p(2 \times 4)$ structure. In each case, P denotes a disordered configuration of dimers.

cal calculations are not accurate enough to distinguish between the $p(2 \times 2)$ and $c(4 \times 2)$ geometries. Changes in the energy of a few millielectronvolts can turn the $c(4 \times 2)$ structure into the ground state with a similar transition temperature to the paramagnetic phase. In any case, our calculations predict that the pure 2×1 geometry is not the ground state and that higher-order reconstructions of either $p(2 \times 2)$ or $c(4 \times 2)$ should be present at low temperatures.

For the " $c(2 \times 2)$ " family, the situation is much clearer. Figure 2(b) predicts a second-order transition between ferromagnetic $c(2 \times 2)$ and paramagnetic (disordered) phases at ~ 800 K. It is tempting to suggest that the large changes in desorption rates recently observed in surface ionization experiments on Si(100) around 980 K may be related to this phase transition.²² Since the results are still preliminary, however, further experiments and careful interpretations are necessary to draw definite conclusions.

Determination of ordered structures and phase diagrams leads to the issues of critical phenomena, encapsulated in the critical exponent values. The second-order transitions here between the ferromagnetic and antiferromagnetic phase and the disordered phase are in the two-dimensional Ising universality class. Accordingly, the correlation length exponent ν and the order-parameter exponent β have the values of 1 and $\frac{1}{8}$, and may

be observable from a careful analysis of diffraction spot widths and intensities, respectively.

In conclusion, at very low T , the " (2×1) " family will most likely give rise to $p(2 \times 2)$ or $c(4 \times 2)$ higher-order spots. Around room temperature these higher-order spots will be lost because of the transition to the disordered phase. The (2×1) spots will persist, however, since the huge dimerization energy of 1.7 eV assures the integrity of the dimers. If a domain of the $c(2 \times 2)$ structure is created, it will undergo a phase transition to the paramagnetic phase at very high temperatures.

We should like to thank A. N. Berker and D. Andelman for many helpful discussions. This work was supported in part by the U. S. Joint Services Electronics Program under Contract No. DAAG-29-83-K003. One of us (J.D.J.) should like to thank the J. S. Guggenheim Foundation for a fellowship.

(a) Present address: Bell Laboratories, Murray Hill, N.J. 07974.

¹D. J. Chadi, Phys. Rev. Lett. 43, 43 (1979).

²Y. Wang and J. D. Joannopoulos, J. Vac. Sci. Technol. 17, 997 (1980); P. Vogl, H. P. Hjalmeron, and J. D. Dow, J. Phys. Chem. Solids 44, 364 (1983).

³D. Vanderbilt and J. D. Joannopoulos, Solid State Commun. 35, 535 (1980), and Phys. Rev. Lett. 49, 823 (1982).

⁴M. T. Yin and M. L. Cohen, Phys. Rev. Lett. 45, 1004 (1980), and Phys. Rev. B 24, 2303 (1981).

⁵J. Ihm and J. D. Joannopoulos, Phys. Rev. B 24,

4191 (1981), and Phys. Rev. Lett. 47, 679 (1981).

⁶W. A. Goddard, III, and T. C. McGill, J. Vac. Sci. Technol. 16, 1308 (1979).

⁷K. C. Pandey, Phys. Rev. Lett. 49, 223 (1982).

⁸A. K. Ray, S. B. Trickey, and A. B. Kunz, Solid State Commun. 41, 351 (1982).

⁹K. G. Wilson, Phys. Rev. B 4, 3174, 3184 (1971).

¹⁰J. M. van Leeuwen, Phys. Rev. Lett. 34, 1056 (1975).

¹¹*Phase Transitions and Critical Phenomena*, edited by C. Domb and M. S. Green (Academic, New York, 1976), Vol. 6.

¹²See, for example, F. Himpsel, P. Heimann, T. Chiang, and D. Eastman, Phys. Rev. Lett. 45, 1112 (1980); P. Koke and W. Monch, Solid State Commun. 36, 1007 (1980); J. Rowe and S. Christman, J. Vac. Sci. Technol. 17, 220 (1980); M. Aono, Y. Hou,

C. Oshima, and Y. Ishizawa, Phys. Rev. Lett. 49, 567 (1982).

¹³R. E. Schlier and H. E. Farnsworth, J. Chem. Phys. 30, 917 (1959).

¹⁴J. J. Lander and J. Morrison, J. Chem. Phys. 37, 729 (1962).

¹⁵S. J. White and D. P. Woodruff, Surf. Sci. 64, 131 (1977).

¹⁶T. D. Poppendick, T. C. Ngoc, and M. B. Webb, Surf. Sci. 75, 287 (1978).

¹⁷S. Y. Tong and A. L. Maldonado, Surf. Sci. 78, 459 (1978).

¹⁸M. J. Cardillo and G. E. Becker, Phys. Rev. B 21, 1497 (1980).

¹⁹F. Jona, H. D. Shih, D. W. Jepsen, and P. M. Marcus, J. Phys. C 12, 1455 (1979).

²⁰T. Ichikawa and S. Ino, Surf. Sci. 85, 22 (1979).

²¹Spin waves in the effective Hamiltonian (phonons in the real system) are neglected because the potential barrier for flipping dimers is about 200 meV.

²²E. F. Greene, private communication; E. F. Greene, J. T. Keeley, and M. A. Pickering, Surf. Sci. 120, 103 (1982).